CFD Letters 15, Issue 7 (2023) 92-111

CFD Letters

Journal homepage:
https://semarakilmu.com.my/journals/index.php/CFD_Letters/index
ISSN: 2180-1363

Magnetohydrodynamic Effect in Mixed Convection Casson Hybrid Nanofluids Flow and Heat Transfer over a Moving Vertical Plate

Norsyasya Zahirah Mohd Zukri[1], Mohd Rijal Ilias[1], Siti Shuhada Ishak[1], Roselah Osman[1,*], Nur Asiah Mohd Makhatar[1], Mohd Nashriq Abd Rahman[2]

[1] School of Mathematical Sciences, College of Computing, Informatics and Media, Universiti Teknologi MARA, 40450 Shah Alam, Selangor, Malaysia
[2] Jabatan Meteorologi Malaysia, Jalan Sultan, 46667 Petaling Jaya, Selangor, Malaysia

ARTICLE INFO

Article history:
Received 11 August 2022
Received in revised form 13 September 2022
Accepted 10 October 2022
Available online 1 July 2023

Keywords:
Magnetohydrodynamics (MHD); Convective Boundary Conditions; Casson Hybrid Nanofluids; Moving Vertical Plate; Nanoparticles Shape

ABSTRACT

The current study examined the effect of nanoparticles shapes on magnetohydrodynamics (MHD), Casson hybrid nanofluids flow, and heat transfer over a moving vertical plate with convective boundary condition. In this study, a base fluid (water) was infused with silver (Ag) and titanium oxide (TiO_2). Similarity transformation techniques are used to convert the partial differential equations of Casson hybrid nanofluids to an ordinary differential equation, which are then solved numerically by applying the implicit finite difference, Keller box method. The velocity and temperature profiles, skin friction, and Nusselt number of Casson hybrid nanofluids were graphically illustrated and numerically tabulated. The results indicate that platelets have the highest velocity and temperature profiles, followed by cylindrical, bricks, and spherical nanoparticles. It was discovered that as the parameters aligned angle of the magnetic field, magnetic field interaction, mixed convection, Casson hybrid nanofluids, and Biot number increase, the velocity increases while the temperature decreases. As the volume fractions of Ag and TiO_2 nanoparticles increase, the velocity decreases while the temperature increases. Except for the Casson hybrid nanofluids parameter, the skin friction and Nusselt number increase as the aligned magnetic angle, magnetic field interaction, mixed convection, volume fraction of Ag and TiO_2 nanoparticles, and Biot number is increased. For all parameters, the plate with the condition moving with the flow has the highest velocity and Nusselt number, followed by the static and moving against the flow plates. When it comes to temperature and skin friction, the plate that is moving against the flow has the highest temperature, followed by the plate that is static and moving along the plate. The findings of this work will contribute to the corpus of knowledge in mathematics by providing fresh information for mathematicians interested in future research on Casson hybrid nanofluids.

1. Introduction

Nanotechnology has been widely used in many varieties of industrial applications. This growing interest received significant interest among researchers over past few years. Basically, nanoparticles

[*] *Corresponding author.*
E-mail address: roselah_osman@uitm.edu.my (Roselah Osman)

https://doi.org/10.37934/cfdl.15.7.92111

are between 1 and 100 nm in sizes and usually composed of oxides, nanotubes, and metals. According to Anwar *et al.,* [1], nanotechnology can design numerous new instruments and materials with a vast variety of applications, such as, energy production, biosensors, chemical industry, nanomedicine, tissue engineering as well as agriculture. One of the main parts of nanotechnology is nanofluids. The inventions of nanofluids not only improve the augmented heat transfer rate but also upgrades the lubrication, tribological and cooling features of ordinary traditional fluid.

Nanofluids has a formation between some conventional fluids such as water, kerosene oil, alcohol, or blood, and between solid nanoparticles. There are limitations to improving the performance of traditional heat transfer fluids, such as water, oil, and Ethylene Glycol mixtures due to the low thermal conductivity of the fluids. Sheikholeslami and Ganji [2] state that there is a strong determination among researchers to develop advanced heat transfer fluids with higher conductivity. Ghosh and Mukhopadhyay [3] mentioned that nanofluid has been used in many energy systems, such as cooling of nuclear systems, radiators, natural convection in enclosures, drawing of copper wires, continuous stretching of plastic films, artificial fibres, hot rolling, etc. Bahiraei *et al*., [4] showed that the higher thermal conductivity of nanofluids compared to ordinary liquids results in lower thermal resistance, and hence, leads to more significant heat transfer rates.

The idea of using hybrid nanofluids is to further improve the heat transfer and pressure drop characteristics by trade-off between advantages and disadvantages of individual suspension, attributed to good aspect ratio, better thermal network and synergistic effect of nanomaterials. Hybrid nanofluids are the solid suspensions of the composite nanoparticles into base fluids [5]. By adding metallic nanoparticles to the base fluids, Manjunatha *et al.,* [6] found a significant improvement in thermal conductivity for the case of stretching sheet. Akbar *et al.,* [7] theoretically investigated a heat performance in a horizontal tube by considering a hybrid nanofluids (alumina and titania) suspended in water. It was found that heat transfer enhancement increases by increasing of hybrid nanofluid volume concentration and volume flow rate. Recently, the study of hybrid nanofluids on flow over various situations was considered by researchers, such as over a vertical, solid sphere, stretching/shrinking sheet, bioconvection and others [8-17].

Besides, Casson fluid is also used to improve the heat transfer performance. Casson fluid is one of the non-Newtonian fluids. Non-Newtonian fluids have been always on researchers' main focus because of their special properties compared to simple Newtonian fluids. Honey, jelly, concentrated fruit juices, soup, human blood, and sauce are in the classification of polar fluid theories which is under the Casson fluid category. There are vast of application of Casson fluid such as in food processing, drilling operations, and bio-engineering operations [18]. Yusuf *et al.,* [19] examined energy effect on a stagnation point slippery MHD Casson nanofluid flow with entropy generation and melting heat transfer. The magnetic field is seen to have majorly affect the viscosity of the molecular. It found that Casson fluid has superior heat transfer characteristics compared to Newtonian fluid. Parandhama *et al.,* [20] used the shooting method to study the effects of numerous physical quantities like dissipation, thermal radiation, and an induced magnetic field on magnetohydrodynamic Casson fluid flow through a vertical plate. They found that Casson fluid velocity decreased with an increase of Casson fluid, magnetic parameter, Soret number, Prandtl number and magnetic Prandtl number. In 2022, Bosli *et al*., [21] investigate the Casson nanofluid over a vertical plate with the effect of an aligned magnetic field and convective boundary condition. It was found that the Casson parameter have increased the velocity profile and heat transfer while the temperature and skin friction has decreased. Meanwhile, Ramakrishna *et al*., [22] explore Casson fluid with the effect of chemical reaction, Soret and Lorentz force past an exponentially accelerated vertical plate using Laplace transform method. They discovered that the increment of Casson parameter led to the reduction in velocity and for the large values of the Casson parameter, the fluid was near to the Newtonian fluid. Others researcher study about unsteady situation in Casson fluid with the impact of magnetic parameter, thermal radiation, and Dufour parameter over the velocity, temperature, and concentration profiles of the fluid by Sulochana and Poornima [23], Rawi *et al.,* [24], Kodi and Mopuri [25], Anwar *et al.,* [26] and El-Zahar *et al.,* [27].

There are different factors that can correlate to the thermal conductivity improvement of nanofluids such as volume fraction, material type, size, and shape [28]. Ellahi *et al.,* [29] and Rao [30] stated that the shape of the nanoparticles may be a lamina, platelet, sphere, or disc. Based on study done by Eastman *et al.,* [31], due to the increased thermal conductivity of copper nanoparticles, the heat transfer also increased. Rashid and Ibrahim [32] found that the lamina shape nanoparticles improve the heat transfer more than other shapes of nanoparticles. According to these results, the heat transfer performance of spherical nanoparticles was the lowest. Hosseinzadeh *et al*., [33] study the three different base fluids with the influence of the magnetic parameter, the nanoparticle volume fraction, micropolar parameter and nanoparticles shape factor over vertical plate. The results indicate that for water-based fluids, the temperature profile of lamina-shaped nanoparticles is 38.09% higher than that of brick-shaped nanoparticles. Bosli *et al*., [21] also study on nanoparticle shape and found that the highest velocity and temperature is laminar shape while the spherical shape has the lowest for all parameters in their study. Then, study nanoparticle shape effects with mixed convective flow along a vertical impermeable wall in a non-Darcy porous medium by Hemalatha and Peri [34]. They discovered that blade shaped nanoparticles have a higher velocity than brick shaped particles. Studies have been done regarding the effect of nanoparticle shape in different situations by Dawar *et al.,* [35], Khashi'ie *et al.,* [36] and Khan *et al.,* [37].

Magnetohydrodynamics (MHD) is known as the study of the magnetic properties and behaviour of electrically conducting fluids. The numerical studies of MHD flow and heat transfer have gained huge concern in recent decades due to their numerous applications in engineering, such as nuclear reactors, aerospace engineering and chemical processing equipment [38]. Babu and Yuvaraj [39] have carried out an investigation regarding MHD steady stokes flow by Navier-Stokes equations as numerical analysis and parallel porous plates with an angular velocity. They found that viscosity is one factor that influence the velocity and temperature characteristics of fluid flow. According to Ilias *et al.,* [40], aligned MHD have significance effect to ferrofluids especially on the heat transfer rates. After that, Ilias *et al.,* [41] analysed the influences of convective boundary condition on the magnetic nanofluids over a flat vertical plate with the presence of a magnetic field. They found that the aligned magnetic field parameter influences the total magnetic interaction parameter. The value of the aligned magnetic field has a huge impact on velocity, temperature, skin friction coefficient, and Nusselt number. In 2022, Rosaidi *et al*., [42] investigate a magnetic field effect of nanofluids over a moving vertical plate with convective boundary conditions. They found that, the plate moving along with the flow provided more heat transfer than the other two cases. Nayan *et al*., [43] explore the aligned MHD flow of a hybrid nanofluid through a porous medium across a vertical plate. Using the Keller box method, Ilias *et al.,* [44] and Ilias [45] studied the heat transfer rate of an MHD flow with free convection effect. The study found that, for both unsteady and steady fluid flow cases, increasing nanoparticle volume fraction and magnetic field strength increased the Nusselt number. The study on MHD effect was discovered in different situation and different by some researchers and founds that the influence of magnetic improve the velocity profiles, skin friction and Nusselt number [46-49].

Mixed convection flow and heat transfer within various geometries have many engineering applications. Investigation of such a problem is important in enhancing the performance of the cooling of electric, electronic and nuclear devices and controlling the fluid flow and heat exchange of solar thermal operations and thermal storage. Hussain *et al.,* [50] explained that mixed convective flow over a permeable or impermeable surface has an important role in manufacturing industries. According to Zhou *et al.,* [51], the convective transfer coefficient is usually considered to be uniform, but it may vary over the cooling surface. Yacob *et al.,* [52] examined the mixed convection flow close to a stretching vertical sheet in a nanofluids. Nanofluids containing Titania nanoparticles improved heat transfer rates compared to the convectional fluid. MHD mixed convection flow across a non-isothermal permeable plate was studied by Prasad *et al.,* [53].

The aim of this research is to expand the study from Bosli *et al.,* [21] to Casson hybrid nanofluids with moving plate conditions. The model used in this study is Tiwari and Das [54]. This study also investigated the effect of different nanoparticles shapes to the velocity and temperature profiles as well as the numerical results on the skin friction coefficient and Nusselt number.

2. Mathematical Formulation

The mathematical model is considered under the following assumptions and conditions [21]:
(i) Two-Dimensional laminar steady flow;
(ii) Boundary layer approximation;
(iii) Non-Newtonian Casson hybrid nanofluids;
(iv) Aligned Magnetohydrodynamics (MHD);
(v) Nanoparticles shape factor;
(vi) Convective boundary conditions;

The rheological equation of state for an isotropic and incompressible flow of Casson hybrid nanofluids is

$$\tau_{ij} = \begin{cases} \left(\mu_B + p_y/\sqrt{2\pi}\right)2e_{ij} & , \quad \pi > \pi_c \\ \left(\mu_B + p_y/\sqrt{2\pi_c}\right)2e_{ij} & , \quad \pi < \pi_c \end{cases}$$

where μ_B is plastic dynamic viscosity of non-Newtonian fluid, p_y is yield stress, π_c is critical value of this product based on the non-Newtonian model and π is the product of the component of deformation rate with itself, namely $\pi = e_{ij}e_{ij}$, e_{ij} is the $(i,j)^{th}$ component of deformation rate. The plate is moving with constant velocity $U_w = \varepsilon U_\infty$, where U_w is the plate velocity, ε is the plate velocity parameter and x and y are the coordinates system measured along the moving plate. An aligned magnetic field with an acute angle, α as shown in Figure 1 is applied to the flow. It is recognized as the origin function as expressed by $B(x) = \frac{B_0}{\sqrt{x}}$ with $B_0 \neq 0$.

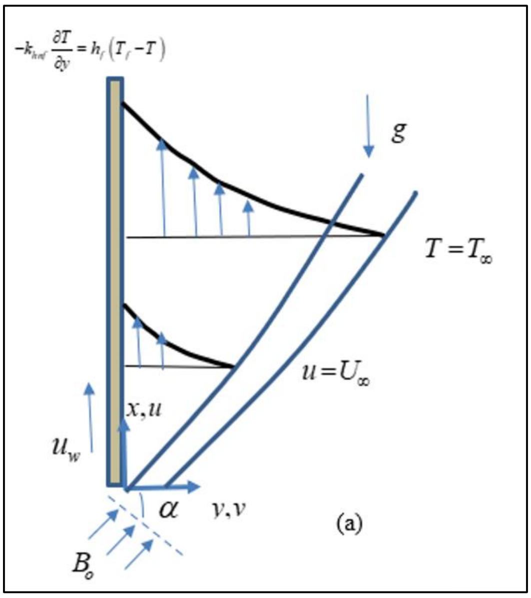

Fig. 1. Physical model for vertical plate

The strength of the magnetic field is represented by denote B_0 and (x, y) is the coordinate along the plate. It is assumed that the base fluid is water, and the nanoparticles are Ag and TiO_2 are in thermal equilibrium. Assuming that the flow in the laminar boundary layer is two-dimensional and steady. Based on Bosli *et al.,* [21], the governing equations are given as:

$$\frac{\partial u}{\partial x}+\frac{\partial v}{\partial y}=0 \tag{1}$$

$$u\frac{\partial u}{\partial x}+v\frac{\partial u}{\partial y}=\frac{\mu_{hnf}}{\rho_{hnf}}\left(1+\frac{1}{\beta_c}\right)\frac{\partial^2 u}{\partial y^2}+\frac{(\rho\beta)_{hnf}}{\rho_{hnf}}g(T-T_\infty)-\frac{\sigma B^2(x)}{\rho_{hnf}}sin^2\alpha(u-U_\infty) \tag{2}$$

$$u\frac{\partial T}{\partial x}+v\frac{\partial T}{\partial y}=\alpha_{hnf}\frac{\partial^2 T}{\partial y^2} \tag{3}$$

While the boundary conditions used in this study are as follows:

$$\begin{aligned} &u=u_w=\varepsilon U_\infty, \quad v=0, \quad -k_{hnf}\frac{\partial T}{\partial y}=h_f\left(T_f-T\right), \quad on\ y=0 \\ &u\to U_\infty, \quad T\to T_\infty \quad as\ y\to\infty \end{aligned} \tag{4}$$

where u is the fluid velocity and v is the normal velocity components along the *x*-axis and *y*-axis. α is the angle of magnetic field, T is the temperature of the fluids, T_f is the nanofluids temperature, T_∞ is the free stream temperature, g is the gravity acceleration, U_∞ is the free stream velocity, ρ_{hnf} is the effective density, σ is the electrical conductivity, $(\rho\beta)_{hnf}$ is the thermal expansion coefficient, μ_{hnf} is the effective dynamic viscosity, α_{hnf} is the thermal diffusivity of the fluid, $\left(\rho C_p\right)_{hnf}$ is the heat capacity of the fluid, k_{hnf} is the thermal conductivity of the hybrid nanofluids, M is the magnetic parameter, h_f is the heat transfer coefficient of fluid $\left(h_f=\frac{c}{\sqrt{x}}, c \text{ is a constant}\right)$, and β_c is the Casson hybrid nanofluids parameter. Table 1 displays the thermophysical relations in nanoparticles shape of hybrid nanofluids [3,21,55].

Different shapes have a different numerical shape factor. This shape factor determines whether the shape is suitable enough with the nanoparticles. m in the thermal conductivity from Table 1 is representing the shape factor and its numerical shape factor and its numerical values for different kind of shapes are shown in Table 3. Shape factor, $m=\frac{3}{Z}$ should be noted, where Z is the sphericity. Sphericity is the ratio of the surface area of the sphere as well as the surface area of the real particles with equal volumes. Sphericity of sphere, platelet, cylinder, and brick are 1.000, 0.526, 0.625, and 0.811, respectively. The shape factor of the particle is 3 which is $m=3$ when The Hamilton-Crosser model becomes a Maxwell-Garnett model. The shape factor m is obtained from Refs. [1,56]. Table 2 shows the thermophysical properties of base fluid which is water and nanoparticles taken from Krishna *et al.,* [57] while Table 3 represents the nanoparticles shape factors (m) by Babu and Yuvaraj [39] and Ilias *et al.,* [40]. The nanoparticles that will be used in this current research are (Ag - Silver) and (TiO_2 – Titanium Oxide).

Table 1
Thermophysical Relation in Nanoparticles Shape of Hybrid Nanofluids [3,21,55]

Properties	Hybrid Nanofluids	
Density	$\rho_{hnf}=(1-\phi_2)\left[(1-\phi_1)\rho_f+\phi_1\rho_{s1}\right]+\phi_2\rho_{s2}$	(5)
Heat Capacity	$(\rho C_p)_{hnf}=(1-\phi_2)\left[(1-\phi_1)(\rho C_p)_f+\phi_1(\rho C_p)_{s1}\right]+\phi_2(\rho C_p)_{s2}$	(6)
Viscosity	$\mu_{hnf}=\dfrac{\mu_f}{(1-\phi_1)^{2.5}(1-\phi_2)^{2.5}}$	(7)
Thermal Conductivity	$\dfrac{k_{hnf}}{k_{bf}}=\dfrac{k_{s2}+(m-1)k_{bf}-(m-1)\phi_2(k_{bf}-k_{s2})}{k_{s2}+(m-1)k_{bf}-\phi_2(k_{bf}-k_{s2})}$	(8)
	$\dfrac{k_{bf}}{k_f}=\dfrac{k_{s1}+(m-1)k_f-(m-1)\phi_1(k_f-k_{s1})}{k_{s1}+(m-1)k_f-\phi_1(k_f-k_{s1})}$	(9)
	$k_{bf}=\dfrac{k_{s1}+(m-1)k_f-(m-1)\phi_1(k_f-k_{s1})}{k_{s1}+(m-1)k_f-\phi_1(k_f-k_{s1})}\times k_f$	
	$\dfrac{k_{hnf}}{k_f}=\dfrac{k_{hnf}}{k_{bf}}\times\dfrac{k_{bf}}{k_f}=\dfrac{k_{s2}+(m-1)k_{bf}-(m-1)\phi_2(k_{bf}-k_{s2})}{k_{s2}+(m-1)k_{bf}-\phi_2(k_{bf}-k_{s2})}\times\dfrac{k_{s1}+(m-1)k_f-(m-1)\phi_1(k_f-k_{s1})}{k_{s1}+(m-1)k_f-\phi_1(k_f-k_{s1})}$	
	where	
	$\dfrac{k_{bf}}{k_f}=\dfrac{k_{s1}+(m-1)k_f-(m-1)\phi_1(k_f-k_{s1})}{k_{s1}+(m-1)k_f-\phi_1(k_f-k_{s1})}$	
Thermal Expansion Coefficient	$\beta_{hnf}=(1-\phi_2)\left[(1-\phi_1)\beta_f+\phi_1\beta_{s1}\right]+\phi_2\beta_{s2}$	(10)
	$(\rho\beta)_{hnf}=(1-\phi_2)\left[(1-\phi_1)(\rho\beta)_f+\phi_1(\rho\beta)_{s1}\right]+\phi_2(\rho\beta)_{s2}$	(11)
Thermal Diffusivity	$\alpha_{hnf}=\dfrac{k_{hnf}}{(\rho C_p)_{hnf}}$	(12)

Table 2
Thermophysical Properties of Base Fluid and Hybrid Nanofluids [57]

Properties	Base Fluid (Water)	Ag (Silver)	TiO_2 (Titanium Oxide)
$\rho(kg/m^3)$	997.1	10500	4250
$C_p(J/kgK)$	4179	235	686.2
$k(W/mk)$	0.613	429	8.9538
$\beta \times 10^{-5}$	21	1.89	0.9
Pr	6.20		

Table 3
The Nanoparticles Shape Factors (m) [1,57,58]

Nanoparticles Shape	Shapes	Shape Factor (m)	Sphericity (Z)
Spherical		3.0	1.000
Platelets		5.7	0.526
Cylindrical		4.8	0.625
Bricks		3.7	0.811

The continuity Eq. (1) is satisfied by introducing stream function $\psi(x, y)$ as shown below,

$$u = \frac{\partial\psi}{\partial y}, v = -\frac{\partial\psi}{\partial x} \tag{13}$$

The following similarity variables are introduced to solve the governing Eq. (1) to Eq. (3),

$$\eta = \frac{y}{x}(Re_x)^{\frac{1}{2}}, \qquad \psi = \upsilon_f\sqrt{Re_x}f(\eta), \qquad \theta = \frac{T-T_\infty}{T_f-T_\infty}, \tag{14}$$

where η is the similarity variable, $Re_x = \frac{U_\infty x}{\nu_f}$ refers to Reynolds number, $\upsilon_f = \frac{\mu_f}{\rho_f}$ is kinematic viscosity, $f(\eta)$ and $\theta(\eta)$ indicate the non-dimensional stream function and temperature, respectively.

By substituting Table 1, (13) and (14) into (2) and (3), the following nonlinear systems of ordinary differential equations are obtained:

$$\left(1 + \frac{1}{\beta_c}\right)f'''(\eta) + \frac{A_1A_2}{2}f(\eta)f''(\eta) + A_1A_3\lambda_T\theta(\eta) + A_1Msin^2\alpha\big(1 - f'(\eta)\big) = 0 \tag{15}$$

$$A_4\theta''^{(\eta)} + \frac{Pr}{2}A_5f(\eta)\theta'(\eta) = 0 \tag{16}$$

By respecting to (4), the boundary conditions obtained are as follows:

$$\begin{aligned} &f(0) = 0,\ \ f'(0) = \varepsilon,\ \ \theta'(0) = -Bi\big(1 - \theta(0)\big)\ \ at\ \ y = 0 \\ &f'(\eta) = 1,\ \ \theta(\eta) = 0\ \ as\ \ y \to \infty \end{aligned} \tag{17}$$

The discussions of numerical results are based on the skin friction coefficient, C_f at the surface of the plate and local Nusselt number, Nu_x which are defined as:

$$C_f = \frac{\tau_w}{\rho_f {U_\infty}^2}, \quad Nu_x = \frac{x q_w}{k_f (T_f - T_\infty)} \tag{18}$$

Where ρ_f is the density of nanofluids, τ_w is the shear stress or wall skin friction, q_w is the convective boundary condition and k_f is the thermal conductivity of the nanofluids.

$$\tau_w = \mu_{hnf}\left(1 + \frac{1}{\beta_c}\right)\left(\frac{\partial u}{\partial y}\right)_{y=0}, \quad q_w = -k_{hnf}\left(\frac{\partial T}{\partial y}\right)_{y=0} \tag{19}$$

By substituting (16) and (21) into (20), the solutions obtained are as follows:

$$\frac{C_f}{(Re_x)^{\frac{1}{2}}} = \left(1 + \frac{1}{\beta_c}\right)\frac{1}{A_1} f''(0), \qquad \frac{Nu_x}{(Re_x)^{\frac{1}{2}}} = -A_4 \theta'(0) \tag{20}$$

where,

$$A_1 = (1-\phi_1)^{2.5}(1-\phi_2)^{2.5}, \quad A_2 = (1-\phi_2)\left\{(1-\phi_1) + \phi_1 \frac{\rho_{s1}}{\rho_f}\right\} + \phi_2 \frac{\rho_{s2}}{\rho_f},$$

$$A_3 = (1-\phi_2)\left\{(1-\phi_1) + \phi_1 \frac{(\rho\beta)_{s1}}{(\rho\beta)_f}\right\} + \phi_2 \frac{(\rho\beta)_{s2}}{(\rho\beta)_f}, \qquad A_4 = \frac{k_{hnf}}{k_f}$$

$$A_5 = (1-\phi_2)\left\{(1-\phi_1) + \phi_1 \frac{(\rho C_p)_{s1}}{(\rho C_p)_f}\right\} + \phi_2 \frac{(\rho C_p)_{s2}}{(\rho C_p)_f},$$

$$M = \frac{\sigma {B_0}^2}{\rho_f U_\infty}, \quad \lambda_T = \frac{Gr_x}{{Re_x}^2}, \quad Pr = \frac{\mu_f (C_p)_f}{k_f}, \quad Bi = \frac{c}{k_{hnf}}\left(\frac{\upsilon_f}{U_\infty}\right)^{\frac{1}{2}}, \quad Gr_x = \frac{g\beta_f (T_w - T_\infty) x^3}{{\upsilon_f}^2}$$

3. Numerical Solution

Eq. (15) and Eq. (16) subject to the boundary conditions (17) are solved numerically using Keller-box method as described in the books by Na and Hansen [59] and Cebeci and Bradshaw [60]. The solution is obtained in the following four steps

(i) Reduce Eq. (15) and Eq. (16) to first-order system.
(ii) Write the difference equations using central differences.
(iii) Linearize the resulting algebraic equations by Newton's method and write them in the matrix-vector form.
(iv) Solve the linear system by the block tridiagonal elimination technique.

4. Results and Discussion

The results will be examined in terms of parameter influence. Velocity and temperature profiles as well as skin friction and Nusselt number of spherical shapes of Casson hybrid nanofluids over a moving vertical plate that are affected by the parameters will be exhibited. Tables will be used to show how the parameters utilized in this study affected skin friction and Nusselt number. To check the validity and accuracy of this study, the numerical values of the skin friction coefficient obtained are compared with those of from four other studies, which are Bataller [61], Aziz [62], Ishak *et al.,*

[63] and Ramesh *et al.,* [64], as shown in Table 4 below. The present findings are reported to be in fair agreement, which confirms the precision of the numerical results obtained.

In order to study the effects of the aligned angle of magnetic field, α, interaction of magnetic field, M, volume fraction of nanoparticles, (ϕ_1, ϕ_2), mixed convection parameters, λ_T, Casson parameters, β_c, and Biot numbers, Bi on effects of nanoparticle shape on moving vertical plate, the numerical results are graphically presented in Figure 2 to Figure 7. For the Casson hybrid nanofluids, the Prandtl number taken is 6.2 and fit the nondimensional values as follows for numerical computation, $\alpha = 90°, M = 1, \phi_1 = 0.1, \phi_2 = 0.1, \lambda_T = 0.5, \beta_c = 2$ and $Bi = 0.1$, unless stated otherwise. In this study, m denotes the shape factor which stated in Table 3.

Table 4
Comparison Results of $\theta(0)$ for Different Values of Biot Number (Bi) when $M = 0$, $Pr = 0.72$, and $\lambda_T = 0,0.5$

Bi	$M = 0$, $Pr = 0.72$, and $\lambda_T = 0$					$M = 0$, $Pr = 0.72$, and $\lambda_T = 0.5$	
	Bataller [61]	Aziz [62]	Ishak *et al.,* [63]	Ramesh *et al.,* [64]	Present	Ramesh et *al.,* [64]	Present
0.05	0.1446	0.1447	0.1446	0.1446	0.144660	0.1388	0.138810
0.1	-	0.2528	0.2527	0.2527	0.252756	0.2386	0.238622
0.2	0.4035	0.4035	0.4035	0.4035	0.403520	0.3774	0.377434
0.4	-	0.5750	0.5750	0.5750	0.575012	0.5398	0.539854
0.6	0.6699	0.6699	0.6699	0.6699	0.669914	0.6337	0.633763
0.8	-	0.7302	0.7301	0.7301	0.730168	0.6954	0.695454
1.0	0.7718	0.7718	0.7718	0.7718	0.771821	0.7392	0.739209
5	-	0.9441	0.9441	0.9441	0.944173	0.9323	0.932320
10	0.9712	0.9713	0.9712	0.9712	0.971285	0.9648	0.964825

Figure 2 to Figure 7 show how velocity and temperature profiles change with different values of $\alpha, M, \phi_1, \phi_2, \lambda_T, \beta_c$ and Bi_x, while the numerical value of skin friction coefficient and Nusselt number for nanoparticles shape are shown in Table 5 and Table 6.

Figure 2(a) and Figure 2(b) show the effects of different values of the vertical angle of a magnetic field, α on the velocity and temperature profile for all conditions of the vertical plate. It was observed that for every condition of vertical plate, an increase in α results in the increase of the velocity profiles but a decrease in the momentum boundary layer thickness. This is due increase in applied magnetic field when the α increases cause the Casson hybrid nanofluid to be pushed towards the plate. When $\alpha = 0°$ it indicates that there is no magnetic field and because of the changes in the aligned field position of the magnetic field, it attracts the nanoparticles. For all the conditions of the vertical plate, when α increases, the velocity profiles increase while the temperature profiles decrease. The thermal boundary layer thickness also decreases. As shown in Table 5 and Table 6, the skin friction coefficient and Nusselt number increases, as α increases. The vertical plate that has the highest result for skin friction coefficient is the vertical plate that is moving against the plate, which is 2.083492, while the vertical plate that is moving together with the plate has a Nusselt number of 0.145804.

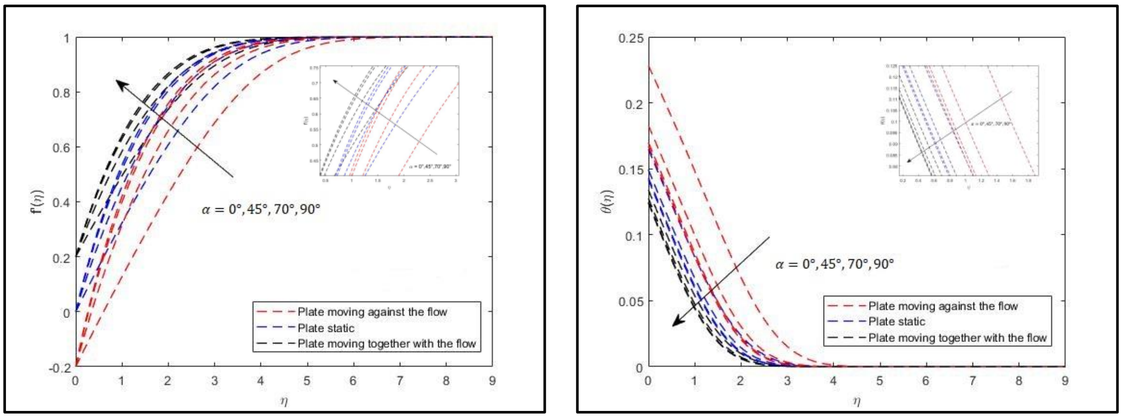

(a) (b)

Fig. 2. Effects of α on (a) velocity profiles and (b) temperature profiles over conditions of vertical plate

Figure 3(a) and Figure 3(b) demonstrates the effect of different values of magnetic field, M on velocity and temperature profiles for all conditions of vertical plate. It is observed that when there is an increase in M, the velocity profiles increase but decline in momentum boundary layer for all conditions of vertical plate. When $M = 0$, this indicates that there is no magnetic force. It means that when the magnetic field value increase, it pushes the fluid towards the plate and thus, the momentum boundary layer decreases. An increase in M leads to an increase in Lorentz force and hence, producing more resistance to the transport phenomena. The temperature profile of all nanoparticles shape and the thermal boundary layer decrease when M increases. For the skin friction and Nusselt number, the value is increasing as M increases as shown in Table 5 and Table 6. The vertical plate that has highest result for skin friction coefficient is the vertical plate that is moving against the plate, which is 3.410252, while for Nusselt number is the vertical plate that is moving together with the plate with 0.147032.

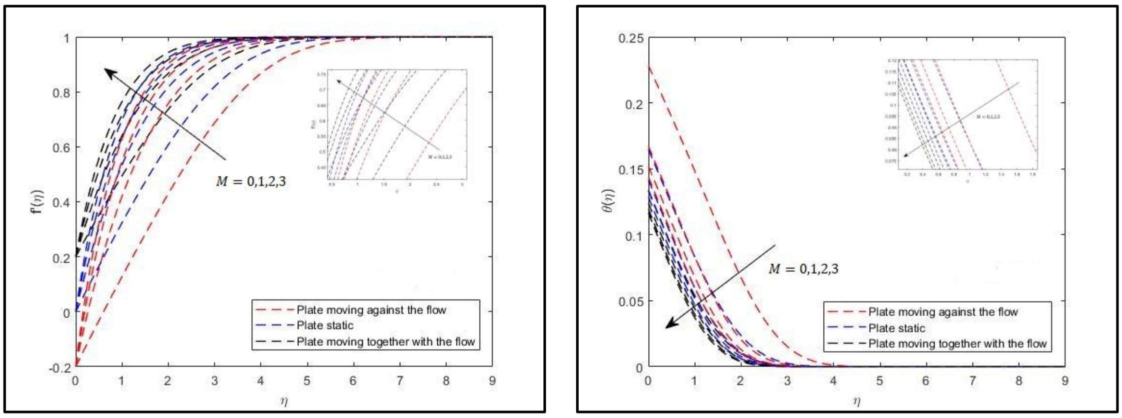

(a) (b)

Fig. 3. Effects of M on (a) velocity profiles and (b) temperature profiles over conditions of vertical plate

Figure 4(a) and Figure 4(b) demonstrate the effect of different values volume fraction of nanoparticle, (ϕ_1, ϕ_2), on velocity and temperature profile for all condition of vertical plate. The increment in (ϕ_1, ϕ_2) makes the velocity profile for all vertical plates decrease but increase in the momentum boundary layer thickness. This accompanies with the enhancement of viscosity that tends the velocity to fall. Then, the temperature increases when (ϕ_1, ϕ_2) increases for all condition of vertical plate. Besides that, the thermal boundary layer thickness also increases with the increase in (ϕ_1, ϕ_2). As shown in Table 5 and Table 6, the skin friction coefficient and Nusselt number increase as (ϕ_1, ϕ_2) increases. It is noticed that vertical plate that is against the flow has the highest skin friction coefficient while for the Nusselt number, vertical plate that is along together with the flow has the highest Nusselt number.

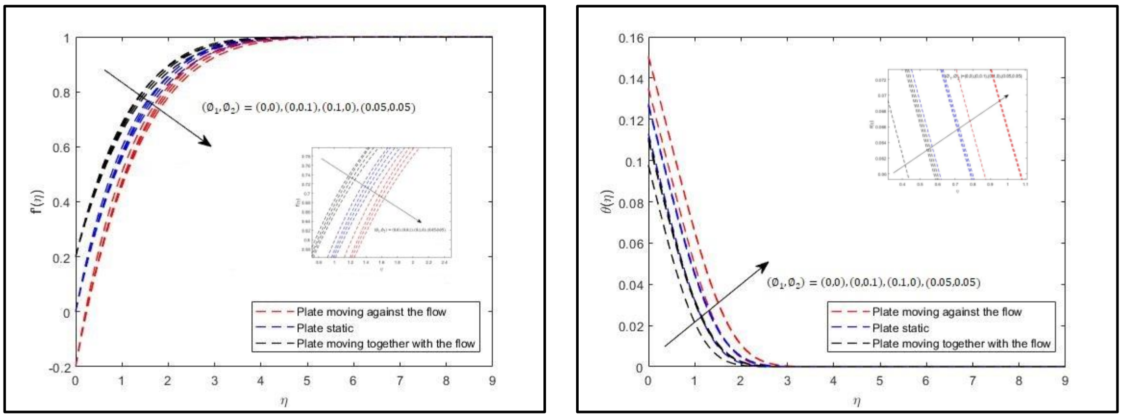

(a) (b)

Fig. 4. Effects of (ϕ_1, ϕ_2) on (a) velocity profiles and (b) temperature profiles over conditions of vertical plate

Figure 5(a) and Figure 5(b) demonstrate the effect of different values of mixed convection parameter, λ_T, on velocity and temperature profile for all condition of vertical plate. It can be observed that when there is increment in λ_T, the temperature profiles and the thermal boundary layer will decrease for all conditions of vertical plate. As shown in Table 5 and Table 6, the skin friction coefficient and Nusselt number increase as λ_T increases. It is noticed that vertical plate that is against the flow has the highest skin friction coefficient while for the Nusselt number, vertical plate that is moving along together with the flow has the highest Nusselt number.

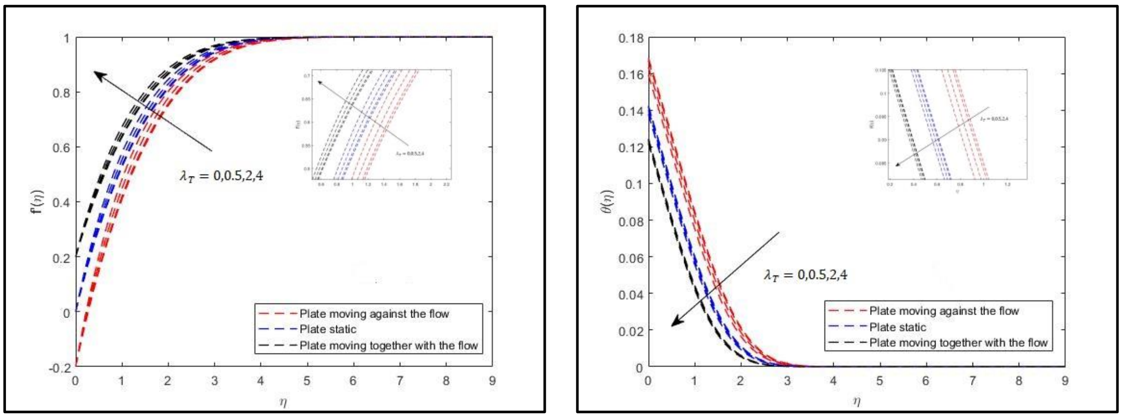

(a) (b)

Fig. 5. Effects of λ_T on (a) velocity profiles and (b) temperature profiles over conditions of vertical plate

Figure 6(a) demonstrates the influence of the Casson hybrid nanofluids parameter, β_c on the nanofluids velocity. The nanofluids velocity increases when β_c increases, while the thickness of boundary layer decreases. It can be explained by when there is increment in the value of β_c, the momentum equation tends to the momentum equation of a Newtonian fluid. Therefore, nanofluids velocity increases as the effective viscous drag force decreases with the increases in β_c. This is explained the reason why the nanofluids velocity reaches the free stream velocity earlier for a greater value of β_c. Figure 6(b) presents the effect of β_c on temperature profiles for all conditions of vertical plate. It is noticeable that fluid temperature decreases with the increment of β_c for all vertical plate's conditions. It is because when β_c increases, it's implying a reduction in yield stress, and therefore, the thickness of the thermal boundary layer reduces. The magnitude of skin friction coefficient is decreases as β_c increases, while Nusselt number is increase as β_c increases for all conditions of vertical plate. As noticed in Table 5 and Table 6, the vertical plate that is against the flow has the highest skin friction coefficient while for the Nusselt number, vertical plate that is along together with the flow has the highest Nusselt number.

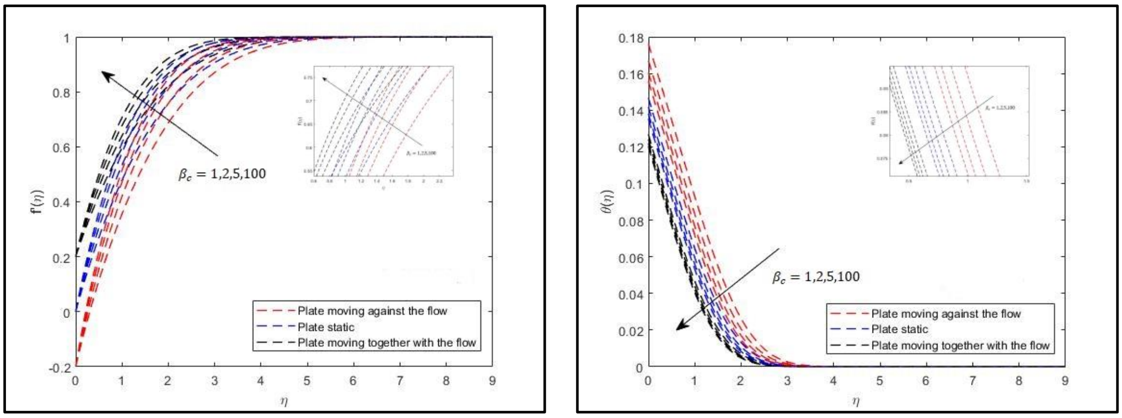

(a) (b)

Fig. 6. Effects of β_c on (a) velocity profiles and (b) temperature profiles over conditions of inclined plate

Based on Figure 7(a), demonstrate the effect of different values of Biot number, Bi_x, on velocity profile for all conditions of vertical plate. The figure shows that when there is an increase in Bi_x, the velocity profiles increases while the momentum boundary layer decreases for all conditions of vertical plate. When $Bi_x = 0$, there is no convective heat transfer and the velocity would also be low, whereas when Bi_x increases, the buoyancy force becomes stronger because of the increase in strength of convective process of the plate. When $Bi_x \to \infty$, this problem become constant wall temperature. Based on Figure 7(b) demonstrates that as Bi_x increases, the temperature profile and the thermal boundary layer also increases. This is because, with an increase in Bi_x, the thermal resistance of the plate decreases and the convective heat transfer of the plate increases.

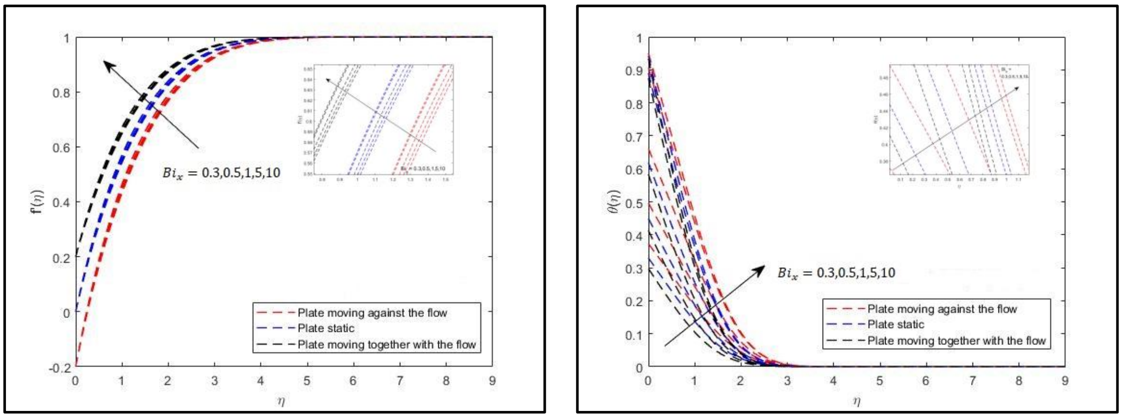

(a) (b)

Fig. 7. Effects of Bi_x on (a) velocity profiles and (b) temperature profiles over conditions of vertical plate

As noticed in Table 5 and Table 6, the vertical plate that is against the flow has the highest skin friction coefficient while for the Nusselt number, vertical plate that is along together with the flow has the highest Nusselt number.

Table 5
Variation of Skin Friction Coefficient at Different Dimensionless Parameters for Conditions of Vertical Plate

α	M	ϕ_1	ϕ_2	λ_T	β_c	Bi_x	Skin Friction Coefficient, $f''(0)$		
							Against the flow	Static	Follow the flow
0°							0.871121	0.857832	0.786728
45°	1	0.1	0.1	0.5	2	0.1	1.591854	1.400844	1.181762
70°							1.979124	1.709013	1.416811
90°							2.083492	1.792991	1.481573
	0						0.871121	0.857832	0.786728
90°	1	0.1	0.1	0.5	2	0.1	2.083492	1.792991	1.481573
	2						2.824873	2.396016	1.951854
	3						3.410252	2.876793	2.330638
		0	0				1.546439	1.306892	1.061974
90°	1	0	0.1	0.5	2	0.1	1.780449	1.512524	1.235132
		0.1	0				1.814574	1.556278	1.282095
		0.05	0.05				1.790127	1.527580	1.252660
				0			2.028175	1.750919	1.448147
90°	1	0.1	0.1	0.5	2	0.1	2.083492	1.792991	1.481573
				2			2.241047	1.915407	1.579958
				4			2.435335	2.070889	1.707094
					1		2.405681	2.068651	1.708520
90°	1	0.1	0.1	0.5	2	0.1	2.083492	1.792991	1.481573
					5		1.863684	1.604723	1.326513
					100		1.709931	1.472930	1.217933
						0.3	2.150792	1.848364	1.528013
						0.5	2.190625	1.883367	1.558840
90°	1	0.1	0.1	0.5	2	1	2.243545	1.932534	1.604125
						5	2.321028	2.010327	1.680748
						10	2.335022	2.025157	1.696082

Table 6
Variation of Nusselt Number at Different Dimensionless Parameters for Conditions of Vertical Plate

α	M	ϕ_1	ϕ_2	λ_T	β_c	Bi_x	Nusselt number, $\theta'(0)$		
							Against the flow	Static	Follow the flow
$0°$							0.128454	0.139014	0.786728
$45°$	1	0.1	0.1	0.5	2	0.1	0.136017	0.141611	0.144139
$70°$							0.138169	0.142618	0.145682
$90°$							0.138639	0.142855	0.145804
	0						0.128454	0.139014	0.144139
$90°$	1	0.1	0.1	0.5	2	0.1	0.138639	0.142855	0.145804
	2						0.141159	0.144227	0.146555
	3						0.142510	0.145035	0.147032
		0	0				0.086500	0.088700	0.090226
$90°$	1	0	0.1	0.5	2	0.1	0.107718	0.110756	0.112869
		0.1	0				0.113116	0.116204	0.118362
		0.05	0.05				0.110530	0.113587	0.115721
				0			0.138409	0.142748	0.145749
$90°$	1	0.1	0.1	0.5	2	0.1	0.138639	0.142855	0.145804
				2			0.139256	0.143152	0.145962
				4			0.139947	0.143508	0.146158
					1		0.137112	0.142027	0.145346
$90°$	1	0.1	0.1	0.5	2	0.1	0.138639	0.142855	0.145804
					5		0.139721	0.143468	0.146156
					100		0.140502	0.143926	0.146425
						0.3	0.313131	0.334667	0.350927
						0.5	0.419385	0.458121	0.488710
$90°$	1	0.1	0.1	0.5	2	1	0.563932	0.634389	0.693459
						5	0.782464	0.920030	1.046174
						10	0.822797	0.975413	1.117701

Table 7 below shows the variation in skin friction coefficient at different dimensionless parameters for shapes of nanoparticles while Table 8 shows the variation of Nusselt number at different dimensionless parameters for shapes of nanoparticles. From both Table 7 and Table 8 below, platelet shape shows the highest skin friction and Nusselt number for all parameters, followed by cylindrical shape, brick shape and lastly spherical shape. The information in the following tables is derived from the static vertical plate condition.

Table 7
Variation in Skin Friction Coefficient at Different Dimensionless Parameters for Shapes of Nanoparticles Over a Vertical Plate

α	M	ϕ_1	ϕ_2	λ_T	β_c	Bi_x	Skin Friction Coefficient, $f''(0)$			
							Shapes of Nanoparticles			
							Spherical	Platelets	Cylindrical	Bricks
0°							0.857832	0.870301	0.866539	0.861422
45°	1	0.1	0.1	0.5	2	0.1	1.400844	1.409309	1.406754	1.403280
70°							1.709013	1.716204	1.714034	1.711083
90°							1.792991	1.799900	1.797815	1.794980
	0						0.857832	0.870301	0.866539	0.861422
90°	1	0.1	0.1	0.5	2	0.1	1.792991	1.799900	1.797815	1.794980
	2						2.396016	2.401407	2.399782	2.397570
	3						2.876793	2.881376	2.879996	2.878115
		0	0				1.306892	1.306892	1.306892	1.306892
90°	1	0	0.1	0.5	2	0.1	1.512524	1.514826	1.514154	1.513210
		0.1	0				1.556278	1.560513	1.559153	1.557422
		0.05	0.05				1.527580	1.530993	1.529929	1.528532
				0			1.750919	1.750919	1.750919	1.750919
90°	1	0.1	0.1	0.5	2	0.1	1.792991	1.799900	1.797815	1.794980
				2			1.915407	1.941835	1.933874	1.923029
				4			2.070889	2.121061	2.105975	2.085385
					1		2.068651	2.076395	2.074057	2.070880
90°	1	0.1	0.1	0.5	2	0.1	1.792991	1.799900	1.797815	1.794980
					5		1.604723	1.611040	1.609134	1.606542
					100		1.472930	1.478821	1.477044	1.474627
						0.3	1.848364	1.862070	1.857980	1.852355
						0.5	1.883367	1.900125	1.895156	1.888278
90°	1	0.1	0.1	0.5	2	1	1.932534	1.952056	1.946312	1.938300
						5	2.010327	2.030798	2.024824	2.016425
						10	2.025157	2.045352	2.039463	2.031177

Table 8
Variation of Nusselt number at Different Dimensionless Parameters for Shapes of Nanoparticles Over a Vertical Plate

α	M	ϕ_1	ϕ_2	λ_T	β_c	Bi_x	Nusselt number, $\theta'(0)$			
							Shapes of Nanoparticles			
							Spherical	Platelets	Cylindrical	Bricks
0°							0.139014	0.181042	0.167804	0.150573
45°	1	0.1	0.1	0.5	2	0.1	0.141611	0.184520	0.171005	0.153413
70°							0.142618	0.185884	0.172256	0.154517
90°							0.142855	0.186206	0.172550	0.154777
	0						0.139014	0.181042	0.167804	0.150573
90°	1	0.1	0.1	0.5	2	0.1	0.142855	0.186206	0.172550	0.154777
	2						0.144227	0.188077	0.174263	0.156285
	3						0.145035	0.189180	0.175272	0.157173
		0	0				0.088700	0.088700	0.088700	0.088700
90°	1	0	0.1	0.5	2	0.1	0.110756	0.124416	0.120354	0.114752
		0.1	0				0.116204	0.140679	0.132579	0.122600
		0.05	0.05				0.113587	0.133658	0.127240	0.119030
				0			0.142748	0.186031	0.172398	0.154653
90°	1	0.1	0.1	0.5	2	0.1	0.142855	0.186206	0.172550	0.154777
				2			0.143152	0.186694	0.172974	0.155123
				4			0.143508	0.187270	0.173475	0.155534
					1		0.142027	0.185055	0.171503	0.153862
90°	1	0.1	0.1	0.5	2	0.1	0.142855	0.186206	0.172550	0.154777
					5		0.143468	0.187059	0.173326	0.155455
					100		0.143926	0.187692	0.173904	0.155960
						0.3	0.334667	0.427935	0.398794	0.360544
						0.5	0.458121	0.578838	0.541297	0.491784
90°	1	0.1	0.1	0.5	2	1	0.634389	0.788333	0.740741	0.677591
						5	0.920030	1.113755	1.054312	0.974836
						10	0.975413	1.174920	1.113771	1.031922

5. Conclusions

The effects of nanoparticle shapes on MHD Casson hybrid nanofluids flow over a moving vertical plate were investigated in this study. A nonlinear PDE is transformed into a dimensionless ODE using the similarity approach and numerically solved using the Keller Box method in Fortran software. Convective boundary conditions were considered in the investigation. The following are the findings of this research:

(i) The increasing value of α, M, λ_T, and β_c,lead to increase the velocity and decrease the temperature.
(ii) When the value of Bi_x increases, the velocity and temperature profiles also increase.
(iii) An increase in (ϕ_1, ϕ_2) depicts a decrement in the velocity profile but a rise in the temperature profiles.
(iv) The skin friction and Nusselt number increase due to the increase in of $\alpha, M, (\phi_1, \phi_2), \lambda_T$, and Bi_x except for β_c.
(v) The condition of plate with the highest skin friction is moving against the flow plate while the highest Nusselt number is the plate that is moving along the flow.
(vi) The nanoparticles shape with the highest velocity and temperature profiles is platelet followed by cylindrical, bricks and spherical shape.

Acknowledgement
The authors extend their appreciation to Universiti Teknologi MARA Shah Alam for funding this work through Lestari SDG-T 5/3 under grant number 600- RMC (137/2019).

References
[1] Anwar, Talha, Poom Kumam, and Phatiphat Thounthong. "A comparative fractional study to evaluate thermal performance of NaAlg-MoS_2-Co hybrid nanofluid subject to shape factor and dual ramped conditions." *Alexandria Engineering Journal* 61, no. 3 (2022): 2166-2187. https://doi.org/10.1016/j.aej.2021.06.085
[2] Sheikholeslami, Mohsen, and Davood Domairry Ganji. *Applications of nanofluid for heat transfer enhancement*. William Andrew, 2017.
[3] Ghosh, Sudipta, and Swati Mukhopadhyay. "MHD slip flow and heat transfer of Casson nanofluid over an exponentially stretching permeable sheet." *International Journal of Automotive and Mechanical Engineering* 14, no. 4 (2017): 4785-4804. https://doi.org/10.15282/ijame.14.4.2017.14.0375
[4] Bahiraei, Mehdi, Ali Monavari, and Hossein Moayedi. "Second law assessment of nanofluid flow in a channel fitted with conical ribs for utilization in solar thermal applications: effect of nanoparticle shape." *International Journal of Heat and Mass Transfer* 151 (2020): 119387. https://doi.org/10.1016/j.ijheatmasstransfer.2020.119387
[5] Tlili, Iskander, Hossam A. Nabwey, M. Girinath Reddy, N. Sandeep, and Maddileti Pasupula. "Effect of resistive heating on incessantly poignant thin needle in magnetohydrodynamic Sakiadis hybrid nanofluid." *Ain Shams Engineering Journal* 12, no. 1 (2021): 1025-1032. https://doi.org/10.1016/j.asej.2020.09.009
[6] Manjunatha, S., B. Ammani Kuttan, S. Jayanthi, Ali Chamkha, and B. J. Gireesha. "Heat transfer enhancement in the boundary layer flow of hybrid nanofluids due to variable viscosity and natural convection." *Heliyon* 5, no. 4 (2019): e01469. https://doi.org/10.1016/j.heliyon.2019.e01469
[7] Akbar, Hanan Mohamad, Asan Suad Mohammed, and Sarah Burhan Ezzat. "Hybrid nanofluid to improve heat transfer and pressure drop through horizontal tube." *Materials Today: Proceedings* 42 (2021): 1885-1888. https://doi.org/10.1016/j.matpr.2020.12.227
[8] Sarkar, Jahar, Pradyumna Ghosh, and Arjumand Adil. "A review on hybrid nanofluids: recent research, development and applications." *Renewable and Sustainable Energy Reviews* 43 (2015): 164-177. https://doi.org/10.1016/j.rser.2014.11.023
[9] Waini, Iskandar, Anuar Ishak, Teodor Groşan, and Ioan Pop. "Mixed convection of a hybrid nanofluid flow along a vertical surface embedded in a porous medium." *International Communications in Heat and Mass Transfer* 114 (2020): 104565. https://doi.org/10.1016/j.icheatmasstransfer.2020.104565
[10] Khashi'ie, Najiyah Safwa, Ezad Hafidz Hafidzuddin, Norihan Md Arifin, and Nadihah Wahi. "Stagnation point flow of hybrid nanofluid over a permeable vertical stretching/shrinking cylinder with thermal stratification effect." *CFD Letters* 12, no. 2 (2020): 80-94.
[11] Mahdy, A., E. R. El-Zahar, A. M. Rashad, W. Saad, and H. S. Al-Juaydi. "The magneto-natural convection flow of a micropolar hybrid nanofluid over a vertical plate saturated in a porous medium." *Fluids* 6, no. 6 (2021): 202. https://doi.org/10.3390/fluids6060202
[12] Ali, I. R., Ammar I. Alsabery, N. A. Bakar, Rozaini Roslan. "Mixed Convection in a Lid-Driven Horizontal Rectangular Cavity Filled with Hybrid Nanofluid By Finite Volume Method." *Journal of Advanced Research in Micro and Nano Engineering* 1, no. 1 (2020): 38-49.
[13] Waini, Iskandar, Anuar Ishak, and Ioan Pop. "Transpiration effects on hybrid nanofluid flow and heat transfer over a stretching/shrinking sheet with uniform shear flow." *Alexandria Engineering Journal* 59, no. 1 (2020): 91-99. https://doi.org/10.1016/j.aej.2019.12.010
[14] Faizal, Nur Faizzati Ahmad, Norihan Md Ariffin, Yong Faezah Rahim, Mohd Ezad Hafidz Hafidzuddin, and Nadihah Wahi. "MHD and slip effect in micropolar hybrid nanofluid and heat transfer over a stretching sheet with thermal radiation and non-uniform heat source/sink." *CFD Letters* 12, no. 11 (2020): 121-130. https://doi.org/10.37934/cfdl.12.11.121130
[15] Rasool, Ghulam, Ali J. Chamkha, Taseer Muhammad, Anum Shafiq, and Ilyas Khan. "Darcy-Forchheimer relation in Casson type MHD nanofluid flow over non-linear stretching surface." *Propulsion and Power Research* 9, no. 2 (2020): 159-168. https://doi.org/10.1016/j.jppr.2020.04.003
[16] Swalmeh, Mohammed Zaki. "Numerical solutions of hybrid nanofluids flow via free convection over a solid sphere." *Journal of Advanced Research in Fluid Mechanics and Thermal Sciences* 83, no. 1 (2021): 34-45. https://doi.org/10.37934/arfmts.83.1.3445
[17] Soid, Siti Khuzaimah, Afiqah Athirah Durahman, Nur Hazirah Adilla Norzawary, Mohd Rijal Ilias, and Amirah Mohamad Sahar. "Magnetohydrodynamic of Copper-Aluminium of Oxide Hybrid Nanoparticles Containing

Gyrotactic Microorganisms over a Vertical Cylinder with Suction." *Journal of Advanced Research in Applied Sciences and Engineering Technology* 28, no. 2 (2022): 222-234. https://doi.org/10.37934/araset.28.2.222234

[18] Sulochana, C., G. P. Ashwinkumar, and N. Sandeep. "Similarity solution of 3D Casson nanofluid flow over a stretching sheet with convective boundary conditions." *Journal of the Nigerian Mathematical Society* 35, no. 1 (2016): 128-141. https://doi.org/10.1016/j.jnnms.2016.01.001

[19] Yusuf, Tunde Abdulkadir, Akaje Wasiu, Sulyman O. Salawu, and Jacob Abiodun Gbadeyan. "Arrhenius activation energy effect on a stagnation point slippery MHD Casson nanofluid flow with entropy generation and melting heat transfer." In *Defect and Diffusion Forum*, vol. 408, pp. 1-18. Trans Tech Publications Ltd, 2021. https://doi.org/10.4028/www.scientific.net/DDF.408.1

[20] Parandhama, A., K. V. S. Raju, and M. Changal Raju. "MHD Casson fluid flow through a vertical plate." *Journal of Computational & Applied Research in Mechanical Engineering (JCARME)* 9, no. 2 (2020): 343-350.

[21] Bosli, Fazillah, Alia Syafiqa Suhaimi, Siti Shuhada Ishak, Mohd Rijal Ilias, Amirah Hazwani Abdul Rahim, and Anis Mardiana Ahmad. "Investigation of Nanoparticles Shape Effects on Aligned MHD Casson Nanofluid Flow and Heat Transfer with Convective Boundary Condition." *Journal of Advanced Research in Fluid Mechanics and Thermal Sciences* 91, no. 1 (2022): 155-171. https://doi.org/10.37934/arfmts.91.1.155171

[22] Ramakrishna, Suresh Babu, Ramesh NL, and Sravan Kumar Thavada. "Effects of chemical reaction, Soret and Lorentz force on Casson fluid flow past an exponentially accelerated vertical plate: A comprehensive analysis." *Heat Transfer* 51, no. 2 (2022): 2237-2257. https://doi.org/10.1002/htj.22398

[23] Sulochana, C., and M. Poornima. "Unsteady MHD Casson fluid flow through vertical plate in the presence of Hall current." *SN Applied Sciences* 1 (2019): 1-14. https://doi.org/10.1007/s42452-019-1656-0

[24] Rawi, N. A., M. R. Ilias, Y. J. Lim, Z. M. Isa, and S. Shafie. "Unsteady mixed convection flow of Casson fluid past an inclined stretching sheet in the presence of nanoparticles." In *Journal of Physics: Conference Series*, vol. 890, no. 1, p. 012048. IOP Publishing, 2017. https://doi.org/10.1088/1742-6596/890/1/012048

[25] Kodi, Raghunath, and Obulesu Mopuri. "Unsteady MHD oscillatory Casson fluid flow past an inclined vertical porous plate in the presence of chemical reaction with heat absorption and Soret effects." *Heat Transfer* 51, no. 1 (2022): 733-752. https://doi.org/10.1002/htj.22327

[26] Anwar, Talha, Poom Kumam, and Wiboonsak Watthayu. "Unsteady MHD natural convection flow of Casson fluid incorporating thermal radiative flux and heat injection/suction mechanism under variable wall conditions." *Scientific Reports* 11, no. 1 (2021): 4275. https://doi.org/10.1038/s41598-021-83691-2

[27] El-Zahar, Essam R., Abd El Nasser Mahdy, Ahmed M. Rashad, Wafaa Saad, and Laila F. Seddek. "Unsteady MHD mixed convection flow of Non-Newtonian Casson hybrid nanofluid in the stagnation zone of sphere spinning impulsively." *Fluids* 6, no. 6 (2021): 197. https://doi.org/10.3390/fluids6060197

[28] Kandasamy, Ramasamy, Nur Atikah bt Adnan, and Radiah Mohammad. "Nanoparticle shape effects on squeezed MHD flow of water based Cu, Al_2O_3 and SWCNTs over a porous sensor surface." *Alexandria Engineering Journal* 57, no. 3 (2018): 1433-1445. https://doi.org/10.1016/j.aej.2017.03.011

[29] Ellahi, R., M. Hassan, and A. Zeeshan. "Shape effects of nanosize particles in Cu-H_2O nanofluid on entropy generation." *International Journal of Heat and Mass Transfer* 81 (2015): 449-456. https://doi.org/10.1016/j.ijheatmasstransfer.2014.10.041

[30] Rao, Yuanqiao. "Nanofluids: stability, phase diagram, rheology and applications." *Particuology* 8, no. 6 (2010): 549-555. https://doi.org/10.1016/j.partic.2010.08.004

[31] Eastman, Jeffrey A., S. U. S. Choi, Sheng Li, W. Yu, and L. J. Thompson. "Anomalously increased effective thermal conductivities of ethylene glycol-based nanofluids containing copper nanoparticles." *Applied Physics Letters* 78, no. 6 (2001): 718-720. https://doi.org/10.1063/1.1341218

[32] Rashid, Umair, and Adnan Ibrahim. "Impacts of nanoparticle shape on Al_2O_3-water nanofluid flow and heat transfer over a non-linear radically stretching sheet." *Advances in Nanoparticles* 9 (2020): 23-39. https://doi.org/10.4236/anp.2020.91002

[33] Hosseinzadeh, Kh, So Roghani, A. Asadi, Amirreza Mogharrebi, and D. D. Ganji. "Investigation of micropolar hybrid ferrofluid flow over a vertical plate by considering various base fluid and nanoparticle shape factor." International Journal of Numerical Methods for Heat & Fluid Flow 31, no. 1 (2020): 402-417. https://doi.org/10.1108/HFF-02-2020-0095

[34] Hemalatha, R., and K. Kameswaran Peri. "Impact of nanoparticle shapes on non-darcy porous medium." *International Communications in Heat and Mass Transfer* 130 (2022): 105777. https://doi.org/10.1016/j.icheatmasstransfer.2021.105777

[35] Dawar, Abdullah, Anwar Saeed, and Poom Kumam. "Magneto-hydrothermal analysis of copper and copper oxide nanoparticles between two parallel plates with Brownian motion and thermophoresis effects." *International Communications in Heat and Mass Transfer* 133 (2022): 105982. https://doi.org/10.1016/j.icheatmasstransfer.2022.105982

[36] Khashi'ie, Najiyah Safwa, Norihan Md Arifin, Mikhail Sheremet, and Ioan Pop. "Shape factor effect of radiative Cu-Al_2O_3/H_2O hybrid nanofluid flow towards an EMHD plate." *Case Studies in Thermal Engineering* 26 (2021): 101199. https://doi.org/10.1016/j.csite.2021.101199

[37] Khan, Umair, Aurang Zaib, Ioan Pop, Sakhinah Abu Bakar, and Anuar Ishak. "Stagnation point flow of a micropolar fluid filled with hybrid nanoparticles by considering various base fluids and nanoparticle shape factors." *International Journal of Numerical Methods for Heat & Fluid Flow* 32, no. 7 (2022): 2320-2344. https://doi.org/10.1108/HFF-07-2021-0445

[38] Chi, Xiaoqing, and Hui Zhang. "Numerical study for the unsteady space fractional magnetohydrodynamic free convective flow and heat transfer with Hall effects." *Applied Mathematics Letters* 120 (2021): 107312. https://doi.org/10.1016/j.aml.2021.107312

[39] Babu, R. Delhi, and V. Yuvaraj. "Magnetohydrodynamic steady stokes flow by Navier-Stokes equations as numerical analysis and parallel porous plates with an angular velocity." *Materials Today: Proceedings* 46 (2021): 3653-3658. https://doi.org/10.1016/j.matpr.2021.01.810

[40] Ilias, Mohd Rijal, Noraihan Afiqah Rawi, and Sharidan Shafie. "MHD free convection flow and heat transfer of ferrofluids over a vertical flat plate with aligned and transverse magnetic field." *Indian Journal of Science and Technology* 9, no. 7 (2016). https://doi.org/10.17485/ijst/2016/v9i36/97347

[41] Ilias, Mohd Rijal, Noraihan Afiqah Rawi, and Sharidan Shafie. "Natural convection of ferrofluid from a fixed vertical plate with aligned magnetic field and convective boundary condition." *Malaysian Journal of Fundamental and Applied Sciences* 13, no. 3 (2017): 223-228. https://doi.org/10.11113/mjfas.v13n3.651

[42] Rosaidi, Nor Alifah, Nurul Hidayah Ab Raji, Siti Nur Hidayatul Ashikin Ibrahim, and Mohd Rijal Ilias. "Aligned magnetohydrodynamics free convection flow of magnetic nanofluid over a moving vertical plate with convective boundary condition." *Journal of Advanced Research in Fluid Mechanics and Thermal Sciences* 93, no. 2 (2022): 37-49. https://doi.org/10.37934/arfmts.93.2.3749

[43] Nayan, Asmahani, Nur Izzatie Farhana Ahmad Fauzan, Mohd Rijal Ilias, Shahida Farhan Zakaria, and Noor Hafizah Zainal Aznam. "Aligned Magnetohydrodynamics (MHD) Flow of Hybrid Nanofluid Over a Vertical Plate Through Porous Medium." *Journal of Advanced Research in Fluid Mechanics and Thermal Sciences* 92, no. 1 (2022): 51-64. https://doi.org/10.37934/arfmts.92.1.5164

[44] Ilias, Mohd Rijal, Ismail N. S'aidah, W. S. Esah, and C. Hussain. "Unsteady aligned MHD boundary layer flow of a magnetic nanofluid over a wedge." *International Journal of Civil Engineering and Technology (IJCIET)* 9 (2018): 794-810.

[45] Ilias, Mohd Rijal. "Steady and Unsteady Aligned Magnetohydrodynamics Free Convection Flows of Magnetic and Non Magnetic Nanofluids along a Wedge, Vertical and Inclined Plates." *PhD diss., Universiti Teknologi Malaysia* (2018).

[46] Ishak, Siti Shuhada, Nurul Nurfatihah Mazlan, Mohd Rijal Ilias, Roselah Osman, Abdul Rahman Mohd Kasim, and Nurul Farahain Mohammad. "Radiation Effects on Inclined Magnetohydrodynamics Mixed Convection Boundary Layer Flow of Hybrid Nanofluids over a Moving and Static Wedge." *Journal of Advanced Research in Applied Sciences and Engineering Technology* 28, no. 3 (2022): 68-84. https://doi.org/10.37934/araset.28.3.6884

[47] Ismail, Nur Suhaida Aznidar, Ahmad Sukri Abd Aziz, Mohd Rijal Ilias, and Siti Khuzaimah Soid. "Mhd boundary layer flow in double stratification medium." In *Journal of Physics: Conference Series*, vol. 1770, no. 1, p. 012045. IOP Publishing, 2021. https://doi.org/10.1088/1742-6596/1770/1/012045

[48] Ilias, Mohd Rijal, Noraihan Afiqah Rawi, and Sharidan Shafie. "Steady aligned MHD free convection of Ferrofluids flow over an inclined plate." *Journal of Mechanical Engineering (JMechE)* 14, no. 2 (2017): 1-15.

[49] Ilias, Mohd Rijal, Ismail N. S'aidah, W. S. Esah, and C. Hussain. "Unsteady aligned MHD boundary layer flow of a magnetic nanofluid over a wedge." *International Journal of Civil Engineering and Technology (IJCIET)* 9 (2018): 794-810.

[50] Hussain, Majid, Abdul Ghaffar, Akhtar Ali, Azeem Shahzad, Kottakkaran Sooppy Nisar, M. R. Alharthi, and Wasim Jamshed. "MHD thermal boundary layer flow of a Casson fluid over a penetrable stretching wedge in the existence of nonlinear radiation and convective boundary condition." *Alexandria Engineering Journal* 60, no. 6 (2021): 5473-5483. https://doi.org/10.1016/j.aej.2021.03.042

[51] Zhou, Long, Mohammad Parhizi, and Ankur Jain. "Theoretical modeling of heat transfer in a multilayer rectangular body with spatially-varying convective heat transfer boundary condition." *International Journal of Thermal Sciences* 170 (2021): 107156. https://doi.org/10.1016/j.ijthermalsci.2021.107156

[52] Yacob, Nor Azizah, Anuar Ishak, Roslinda Nazar, and Ioan Pop. "Mixed convection flow adjacent to a stretching vertical sheet in a nanofluid." *Journal of Applied Mathematics* 2013 (2013). https://doi.org/10.1155/2013/696191

[53] Prasad, K. V., P. S. Datti, and K. Vajravelu. "MHD mixed convection flow over a permeable non-isothermal wedge." *Journal of King Saud University-Science* 25, no. 4 (2013): 313-324. https://doi.org/10.1016/j.jksus.2013.02.005

[54] Tiwari, Raj Kamal, and Manab Kumar Das. "Heat transfer augmentation in a two-sided lid-driven differentially heated square cavity utilizing nanofluids." *International Journal of Heat and Mass Transfer* 50, no. 9-10 (2007): 2002-2018. https://doi.org/10.1016/j.ijheatmasstransfer.2006.09.034

[55] Hayat, Tanzila, and S. Nadeem. "Heat transfer enhancement with Ag-CuO/water hybrid nanofluid." *Results in Physics* 7 (2017): 2317-2324. https://doi.org/10.1016/j.rinp.2017.06.034

[56] Sheikholeslami, M., and M. M. Bhatti. "Forced convection of nanofluid in presence of constant magnetic field considering shape effects of nanoparticles." *International Journal of Heat and Mass Transfer* 111 (2017): 1039-1049. https://doi.org/10.1016/j.ijheatmasstransfer.2017.04.070

[57] Krishna, M. Veera, N. Ameer Ahammad, and Ali J. Chamkha. "Radiative MHD flow of Casson hybrid nanofluid over an infinite exponentially accelerated vertical porous surface." *Case Studies in Thermal Engineering* 27 (2021): 101229. https://doi.org/10.1016/j.csite.2021.101229

[58] Akbar, Noreen Sher, and Adil Wahid Butt. "Ferromagnetic effects for peristaltic flow of Cu-water nanofluid for different shapes of nanosize particles." *Applied Nanoscience* 6 (2016): 379-385. https://doi.org/10.1007/s13204-015-0430-x

[59] Na, Tsung Y., and Arthur G. Hansen. "Similarity analysis of differential equations by Lie group." *Journal of the Franklin Institute* 292, no. 6 (1971): 471-489. https://doi.org/10.1016/0016-0032(71)90167-0

[60] Cebeci, Tuncer, and Peter Bradshaw. *Physical and computational aspects of convective heat transfer*. Springer Science & Business Media, 2012.

[61] Bataller, Rafael Cortell. "Radiation effects for the Blasius and Sakiadis flows with a convective surface boundary condition." *Applied Mathematics and Computation* 206, no. 2 (2008): 832-840. https://doi.org/10.1016/j.amc.2008.10.001

[62] Aziz, Abdul. "A similarity solution for laminar thermal boundary layer over a flat plate with a convective surface boundary condition." *Communications in Nonlinear Science and Numerical Simulation* 14, no. 4 (2009): 1064-1068. https://doi.org/10.1016/j.cnsns.2008.05.003

[63] Ishak, Anuar, Nor Azizah Yacob, and Norfifah Bachok. "Radiation effects on the thermal boundary layer flow over a moving plate with convective boundary condition." *Meccanica* 46 (2011): 795-801. https://doi.org/10.1007/s11012-010-9338-4

[64] Ramesh, G. K., A. J. Chamkha, and B. J. Gireesha. "Boundary layer flow past an inclined stationary/moving flat plate with convective boundary condition." *Afrika Matematika* 27 (2016): 87-95. https://doi.org/10.1007/s13370-015-0323-x